

ORIGINAL

Correlation and Characteristics of Intravoxel Incoherent Motion and Arterial Spin Labeling Techniques Versus Multiple Parameters Obtained on Dynamic Susceptibility Contrast Perfusion MRI for Brain Tumors

Enkh-Amgalan Dolgorsuren¹, MD, Masafumi Harada¹, MD, Ph.D., Yuki Kanazawa², Ph.D., Takashi Abe¹, MD, Ph.D., Maki Otomo¹, MD, Yuki Matsumoto¹, MD, Yoshifumi Mizobuchi³, MD, Ph.D., and Kohhei Nakajima³, MD, Ph.D.

¹Department of Radiology and Radiation Oncology, Tokushima University, Tokushima, Japan, ²Institute of Biomedical Sciences, Tokushima University, Tokushima, Japan, ³Department of Neurosurgery, Tokushima University, Tokushima, Japan

Abstract : Purpose : To compare data on brain tumors derived from intravoxel incoherent motion (IVIM) and arterial spin labeling (ASL) imaging with multiple parameters obtained on dynamic susceptibility contrast (DSC) perfusion MRI and to clarify the characteristics of IVIM and ASL perfusion data from the viewpoint of cerebral blood flow (CBF) analysis. **Methods :** ASL-CBF and IVIM techniques as well as DSC examination were performed in 24 patients with brain tumors. The IVIM data were analyzed with the two models. The relative blood flow (rBF), relative blood volume (rBV) corrected relative blood volume (crBV), mean transit time (MTT), and leakage coefficient (K2) were obtained from the DSC MRI data. **Results :** The ASL-CBF had the same tendency as the perfusion parameters derived from the DSC data, but the permeability from the vessels had less of an effect on the ASL-CBF. The diffusion coefficient of the fast component on IVIM contained more information on permeability than the f value. **Conclusion :** ASL-CBF is more suitable for the evaluation of perfusion in brain tumors than IVIM parameters. ASL-CBF and IVIM techniques should be carefully selected and the biological significance of each parameter should be understood for the correct comprehension of the pathological status of brain tumors. *J. Med. Invest.* 66:308-313, August, 2019

Keywords : Intravoxel incoherent motion, brain tumor, arterial spin labeling, dynamic susceptibility contrast perfusion

INTRODUCTION

Perfusion plays a vital role in brain function and is an essential part of brain metabolism. Perfusion imaging is useful for evaluating tumor blood supply, particularly for the differential diagnosis of tumor stages (1-3) and in prognosis prediction (4) and treatment strategy (5) planning. In addition, perfusion can reflect the microvascular proliferation or angiogenesis of the tumor (1, 6).

Three different methods have been reported to evaluate perfusion on MRI. The most standard method in the clinical setting is dynamic susceptibility contrast (DSC), which is based on continuous time-series measurement after injection of contrast medium. Another is the arterial spin labeling (ASL) technique, which uses radiofrequency pulses to detect blood flow. The final technique is the intra-voxel incoherent motion (IVIM) method, which uses several different strengths of motion-probing gradients, called b -values.

DSC is commonly used to evaluate and differentiate types of brain tumors (7) and is a fundamental technique for brain tumor follow-up (8-10). The DSC method provides many parameters related to perfusion, not only relative blood flow (rBF) and relative blood volume (rBV) in the cerebrum, but also the mean transit time (MTT) and leakage coefficient (K2), which reflect

physiological conditions (7) such as angiogenesis and vascular density (8-12).

Blood flow in the carotid arteries is used as an endogenous tracer for perfusion imaging in the ASL technique, which is the main method applied in non-enhanced perfusion MRI (6, 13). ASL is an advanced and useful technique for assessing intracranial masses and enables differentiation of brain tumor recurrence from its necrosis. Thus, ASL plays a role in monitoring the outcome and progress of tumor treatment (14).

The IVIM procedure concurrently determines perfusion and diffusion parameters of tumors (3, 15-20) without the need for contrast medium (3, 9). This method has major advantages because it is safe, repeatable, quantitative, and independent of arterial input function (3, 16, 19). Although IVIM is used to assess head and neck tumors (5, 19), breast tumors, and other kinds of tumors and diseases (8, 18), its characteristics and differences from other perfusion MRI techniques remain unknown.

The purpose of this study was to compare the IVIM and ASL techniques with various DSC perfusion parameters and to clarify the characteristics and differences of IVIM and ASL perfusion data from those derived by the DSC method.

MATERIALS AND METHODS

The ethics committee of Tokushima University Hospital approved this research, and informed consent was obtained from all patients prior to their enrollment. From September 2015 to March 2017, MRI examinations including ASL, IVIM, and DSC methods were conducted in 24 patients (15 men and 9 women; age, 22–93 years; mean age, 59 ± 34 years) at Tokushima

Received for publication June 18, 2019; accepted June 27, 2019.

Address correspondence and reprint requests to Enkh-Amgalan Dolgorsuren, Department of Radiology and Radiation Oncology, Institute of Biomedical Sciences, The University of Tokushima Graduate School, 3-18-15, Kuramoto-cho, Tokushima city, Tokushima 770-8509, Japan and Fax : +81-88-633-7468.

University Hospital. Of the 24 patients, 13 underwent pathological confirmation. There were 4 cases of glioblastoma, 3 of malignant lymphoma, 3 of oligodendroglioma, and 1 each of anaplastic astrocytoma, pilocytic astrocytoma, and diffuse astrocytoma. The remaining 11 patients were clinically diagnosed without pathological examination as having 7 metastatic brain tumors, 2 malignant lymphomas, and 2 diffuse astrocytomas.

MR IMAGING PROTOCOL

Imaging was performed using a 3-T scanner (Discovery 750; GE Healthcare, Chicago, IL) with a standard 8-channel head coil. All MRI examinations included T2-weighted axial IVIM, ASL, and DSC perfusion MRI.

For the ASL method, the pseudo-continuous labeling technique was used with a 3D spiral fast spin-echo sequence encompassing the whole brain. The settings applied were as follows: 512 sampling points on 8 spirals; field of view (FOV), 24 cm; repetition time, 4635 ms; echo time, 10.5 ms; number of excitations (NEX), 2; reconstructed matrix, 64×64 ; labeling duration, 1650 ms; post-labeling delay, 1525 ms; slice thickness, 4 mm; and number of slices, 36. The total acquisition time was 3 min 15 s. Quantitation of ASL imaging was conducted according to the literature (21) and an ASL-cerebral blood flow (ASL-CBF) map was generated.

DSC MRI was acquired using gradient-echo echo planar imaging as follows: FOV, 24 cm; repetition time, 1990 ms; echo time, 30 ms; reconstructed matrix, 128×128 ; NEX, 1; flip angle, 90° ; slice thickness, 4 mm; number of slices, 20; and total acquisition time, 100 s.

We used a standard diffusion-weighted spin-echo echo planar imaging as the IVIM sequence, with 11 different b-values (10, 20, 30, 40, 60, 80, 100, 200, 400, 800, and 1000 s/mm^2) in three orthogonal directions. The IVIM images were obtained as follows: FOV, 24 cm; repetition time, 4000 ms; echo time, 58.3 ms; slice thickness, 5 mm; number of slices, 25; NEX, 1; and total scan time, 2 min 20 s.

DATA ANALYSIS

IVIM, ASL, and DSC MRI images were examined with Vitrea version 7 (Canon Medical Systems Ltd., Otawara, Japan) based on the Bayesian fitting method. DSC data were obtained using an automated arterial input function (7), which was used for deconvolution of the measured tissue tracer concentration-time curve.

MTT maps are described as the ratio between the rBF and rBV, which is called the tissue response function. The rBF map is the ratio between the rBV and MTT, which is the concentration-time curve. Using the numeric integration of cerebral blood flow values, DSC-rBF maps were created (7,10). The time to peak (TTP) was calculated on DSC MRI and is the time from the injection of the contrast medium to the peak of the signal increase; it reaches its highest concentration in specific areas of interest (22). The leakage or permeability rate, which is useful for DSC tumor imaging, is described by the K2 (11). DSC corrected relative blood volume (crBV) was calculated by the compensation function depending on K2 values.

The IVIM data were obtained using two different models.

(a) The two-component model is expressed by:

$$S/S_0 = f \exp[-bD^*] + (1-f) \exp[-bD]$$

Where D^* is the diffusion coefficient of the fast component, D is the diffusion coefficient of the slow component, f is the ratio of the fast component, b is the b-value, S is the mean diffusion

signal intensity, and S_0 is the mean signal intensity. This value is described as the theory of the water movement, and each map reports different information (23).

(b) The stretched model, which generates DDC and alpha (α), as non-Gaussian diffusion indices, expressed by:

$$S/S_0 = \exp\{-(bc-b_0) \text{DDC}\}^\alpha$$

Where DDC is the distributed diffusion coefficient and alpha is the heterogeneity index ($0 \leq \alpha \leq 1$).

The regions of interest (ROIs) were drawn in the regions of tumors by avoiding hemorrhagic, necrotic, and non-parenchymal areas using T2-weighted and contrast-enhanced T1-weighted imaging (Fig. 1). The ROIs were copied to the ASL, IVIM, and DSC perfusion MRI parameter maps. Circular ROIs with a diameter of 7 mm were additionally measured on normal-appearing white matter (NAWM). The mean values of the ROIs in the tumor were normalized by the ratio divided by the mean values of the ROIs in NAWM.



Fig 1. Oligodendroglioma. 1. Tumor region of interest (ROI). 2. Normal appearing white matter.

STATISTICAL ANALYSIS

All statistical analyses were performed with GraphPad Prism 7.00 (GraphPad Software, Inc., San Diego, CA). Pearson's correlation was used to assess the relationship among IVIM parameters and ASL and DSC perfusion parameters. A p-value of less than 0.05 was considered to be significant.

RESULTS

The representative maps obtained in this study are shown in Figures 2–4. Figure 2 shows the parameter maps derived from ASL, IVIM, and DSC imaging of a patient with glioblastoma. The ASL-CBF map showed high perfusion in the tumor (Fig. 2B), the D map showed inhomogeneous hyperintensity in the tumor (Fig. 2C), the D^* map clearly demarcated the tumor borders as an enhancement image (Fig. 2D), and the f map clearly highlighted an area with high perfusion in the anterior tumor margin (Fig. 2E). High perfusion was detected in the center of the tumor in the rBF (Fig. 2G), rBV (Fig. 2H) and crBV (Fig. 2I) maps. The K2 showed high value in the area of the tumor tissue

(Fig. 2J).

Figure 3 shows various images of a patient with oligodendroglioma. Low perfusion was found in the ASL-CBF map (Fig. 3B), D^* (Fig. 3D), and f (Fig. 3E) maps. rBF (Fig. 3G) and rBV (Fig. 3H) maps showed almost the same tendency as the low perfusion.

Figure 4 shows a patient with malignant lymphoma. The ASL-CBF map (Fig. 4B) revealed the same level in the lymphoma as in the normal white matter. The D^* (Fig. 4D), rBF (Fig. 4G), rBV (Fig. 4H), and $crBV$ (Fig. 4I) maps did not show increased index values in the tumor. The f map showed a moderately high value in the center of the tumor (Fig. 4E).

The results of a comparison of the multiple parameters derived from the IVIM, ASL, and DSC methods are summarized in Table 1. The ASL-CBF map showed a stronger correlation with the DSC- rBF and $crBV$ than the D^* and f values on IVIM. ASL was correlated with the f map on IVIM ($r = 0.414$, $p < 0.05$), rBF ($r = 0.667$, $p < 0.001$), rBV ($r = 0.584$, $p < 0.01$), and $crBV$ ($r = 0.662$, $p < 0.01$), but not with the $K2$. The D^* was correlated with the rBV ($r = 0.604$, $p < 0.01$), $crBV$ ($r = 0.494$, $p < 0.05$),

and $K2$ ($r = 0.581$, $p < 0.01$) and the f was correlated with the $rCBF$ ($r = 0.44$, $p < 0.05$) and rBV ($r = 0.435$, $p < 0.05$), but was only slightly correlated with the $K2$. The D value was strongly correlated with the ADC ($r = 0.992$, $p < 0.0001$) and σ ($r = 0.768$, $p < 0.0001$) but these parameters were not correlated with any DSC parameters. The α on IVIM was negatively correlated with the ASL-CBF map ($r = -0.446$, $p < 0.05$) and the f on IVIM ($r = -0.606$, $p < 0.01$). The ASL-CBF map showed a moderate correlation with the TTP on DSC ($r = 0.535$, $p < 0.05$), but the correlation between the ASL-CBF and $K2$ was weak.

The results of various perfusion parameters compared among high-grade glioma, low-grade glioma, and malignant lymphoma are summarized in Table 2. The mean values of high-grade glioma derived from the ASL-CBF, f , rBF , rBV , and $crBV$ maps were slightly higher than those of low-grade glioma, but there were no significant differences. The mean values of malignant lymphoma derived from the ASL-CBF, rBF , rBV , and $crBV$ maps were lower than those of high-grade glioma, but the differences between the two groups were not significant.

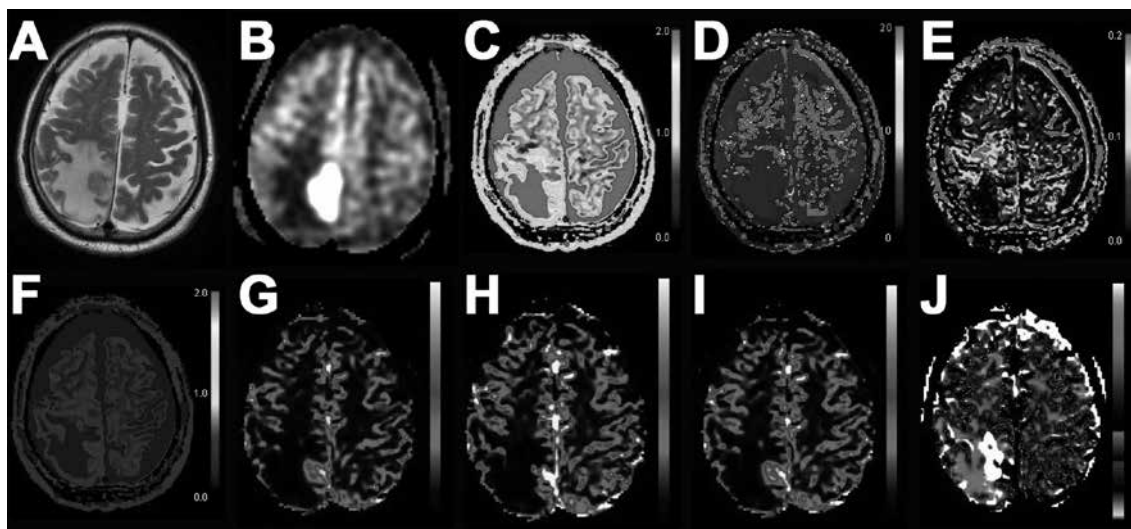


Fig 2. Male, aged 77 years with glioblastoma. T2 weighted image (A), Arterial spin labeling (B), D map (C), D^* map (D), f map (E), ADC map (F), rBF (G), rBV (H), $crBV$ (I), $K2$ (J).

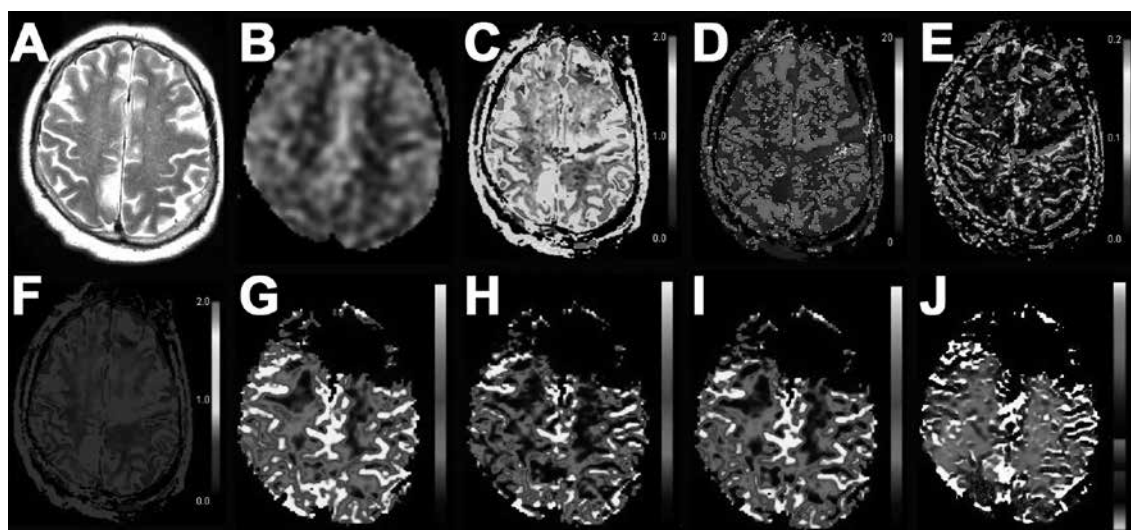


Fig 3. Female, aged 67 years with oligodendroglioma. T2 weighted image (A), Arterial spin labeling (B), D map (C), D^* map (D), f map (E), ADC map (F), rBF (G), rBV (H), $crBV$ (I), $K2$ (J).

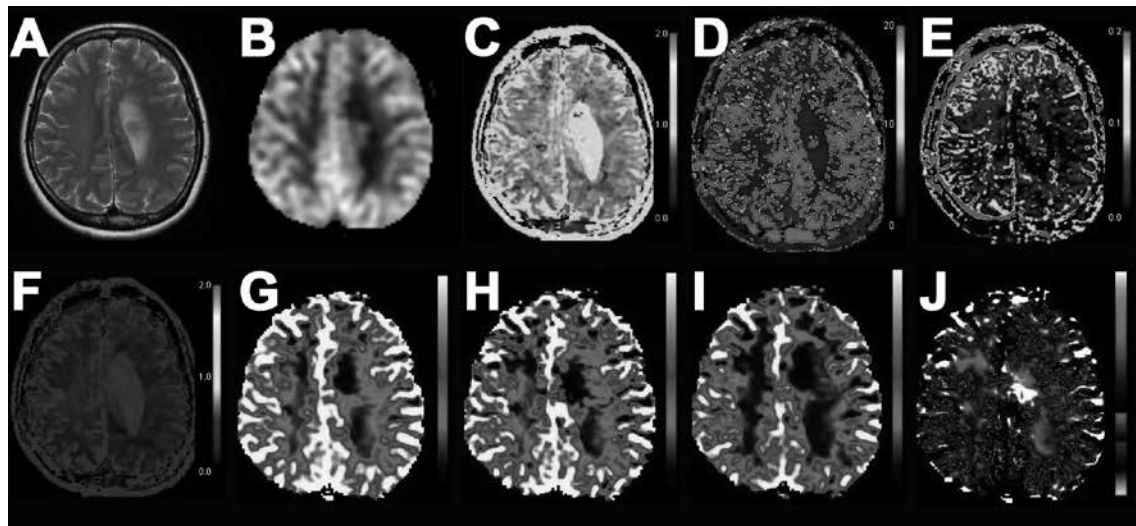


Fig 4. Female, aged 40 years with malignant lymphoma. T2 weighted image (A), Arterial spin labeling (B), D map (C), D*map (D), f map (E), ADC map (F), rBF (G), rBV (H), crBV (I), K2(J).

Table 1. Correlation analysis : DSC and ASL or IVIM

	ASL-CBF	D	D*	f	ADC	alfa	sigma
ASL-CBF	-	-0.139	0.361	0.414*	-0.071	-0.446*	-0.045
rBF	0.667***	0.015	0.382	0.44*	0.147	-0.507*	0.244
rBV	0.584**	0.084	0.604**	0.435*	0.249	-0.371	0.391
crBV	0.662**	0.018	0.494*	0.289	0.111	-0.228	0.19
MTT	-0.332	0.154	0.257	0.0007	0.92	0.157	0.253
Tmax	-0.419	0.122	-0.33	-0.115	0.14	0.169	0.202
TTP	-0.535*	-0.004	-0.205	-0.125	0.022	0.244	0.203
K2	0.344	0.153	0.581**	0.344	0.26	-0.4	0.373
tMIP	0.589**	0.034	0.523*	0.28	0.129	-0.26	0.228

Pearson's rank correlation (no.of cases = 24) **** p < 0.0001 ; *** p < 0.001 ; ** p < 0.01 ; * p < 0.05.

ASL-CBF -arterial spin labeling, D -diffusion coefficient of slow, D* -diffusion coefficient of fast component, f -ratio of the fast component, ADC -apparent diffusion coefficient, rBF -relative cerebral blood flow, rBV -relative cerebral volume, crBV -relative cerebral blood corrected, MTT -mean transit time, Tmax -time to max, TTP -time to peak, K2 -leakage coefficient

Table 2. Comparison of brain tumors

	HGG	LGG	Lymphoma
ASL-CBF	1.22 ± 13.6	1.04 ± 5.41	1.09 ± 8.93
f	2.26 ± 0.12	1.66 ± 0.35	2.56 ± 0.13
D*	0.66 ± 15.8	0.67 ± 12.36	0.80 ± 18.3
rBF	1.92 ± 11.83	1.86 ± 12.15	1.24 ± 6.16
rBV	2.18 ± 2.78	2.04 ± 1.16	1.58 ± 1.20
crBV	2.48 ± 1.00	2.28 ± 0.87	1.58 ± 0.59
MTT	1.16 ± 5.90	0.99 ± 3.03	1.06 ± 3.68
K2	2.09 ± 304.01	3.22 ± 142.02	1.72 ± 77.46

The numeric value is determined by the mean value. (mean value ± standard deviation).

ASL-CBF -arterial spin labeling, D* -diffusion coefficient of fast component, f -ratio of the fast component, rBF -relative cerebral blood flow, rBV -relative cerebral volume, crBV -relative cerebral blood corrected, MTT -mean transit time, K2 -leakage coefficient, HGG -High-grade glioma, LGG -Low-grade glioma.

DISCUSSION

The DSC technique is the most common method for perfusion MRI and is based on multiple theories of arterial input function (24). DSC is often used for brain tumors and can usually identify leakage of the contrast medium in a tumor (25). The K2 parameter can usually be used to reflect permeability, and leakage correction for rBV can be conducted (11, 26) However, the contrast agent is harmful to patients with kidney disease due to the risk of renal failure. Because ASL and IVIM do not require contrast medium, these methods can be used as alternative DSC perfusion MRI techniques for patients with a contraindication to contrast medium. Furthermore, the IVIM method can generate diffusion parameters in addition to visualizing perfusion (5, 6).

In this study, the ASL-rCBF was more strongly correlated with the rBF and crBV on DSC than any other parameter derived from IVIM. Previous studies indicated the highest correlation between ASL and the DSC-rCBF, as well as between ASL and the DSC-rBV, and that these correlations can be affected by the blood flow rate (27). In addition, in this study, we found that

the ASL-rCBF was slightly correlated with the K2 and strongly correlated with the rCBV than the non-corrected rBV. Moreover, the ASL-rCBF showed a moderate correlation with the TTP on DSC. These findings suggest that the ASL-rCBF was less influenced by permeability but included information on the transit time (6, 28, 29).

The D^* and f values on IVIM included some perfusion information that correlated with the DSC-rBV, although the correlation was weaker than with the ASL-CBF. According to a previous study, the f is moderately correlated with the DSC-rBV (8). Similarly, another study (9) reported a moderate positive correlation among the f , DSC-rBF, and rBV. Our results showed that the f , DSC-rCBF, and DSC-rBV were identically correlated with each other. Based on these results, the f value can be used to estimate the vascularity of gliomas and may be correlated with the DSC-rBV on DSC imaging (1, 8, 17). Previous studies suggested that the f value can differentiate high- and low-grade gliomas (1, 8, 23), although we failed to find a significant difference in the f value according to glioma grade, probably due to the small number of subjects.

Our study showed that the permeability reflected by K2 had more influence on the D^* than the f and ASL-CBF. The D^* value is considered to contain more information on permeability due to pathological changes in tumors than the f (3, 6), which cannot be obtained on ASL perfusion data.

The correlation analysis also showed that the alpha value on the stretched model was correlated with the ASL-rCBF and rBF. This finding was considered to indicate that the ASL-CBF and rBF include information on the heterogeneity of blood flow, which deviates from the Gaussian distribution. The extent of the non-Gaussian distribution of blood flow may influence the values of the ASL-CBF and rBF. The D and DDC were not correlated with any perfusion parameters derived from DSC, but the alpha value analyzed by the stretched model was moderately correlated with the DSC-rBF. The D and DDC are independent in terms of perfusion information, but the non-Gaussian effect of IVIM is somewhat related to the rBF (16, 30).

All of the three methods have their own features. DSC MRI is mainly used in clinics for evaluating brain tumor. However, because gadolinium may cause side effects in some people, ASL-CBF can be applicable for patients of contraindication of contrast medium. On the other hand, IVIM imaging simultaneously shows additional information concerning with blood flow such as permeability and diffusion parameters.

This study has some important limitations. We included a small number of patients in our study and half of their tumors had not been pathologically identified. This may be why we failed to find significant differences between high- and low-grade glioma.

In conclusion, the ASL-CBF better reflects tissue perfusion than any other IVIM parameters and is possibly not influenced by permeability. The D^* may contain more information on permeability than the f value. The ASL-CBF and DSC-rBF are slightly correlated with the non-Gaussian extent on IVIM. The differences in these characteristics are important to interpret various perfusion data using different techniques.

CONFLICT OF INTEREST

This study received partial economical support from Bayer Pharmaceutical company.

ACKNOWLEDGEMENTS

We appreciate the cooperation of the Department of Neurosurgery managed by Prof. Yasushi Takagi. This study was supported by a Grant-in-Aid for research from the National Center of Neurology and Psychiatry and cooperated with GE Healthcare Japan.

REFERENCES

1. Togao O, Hiwatashi A, Yamashita K, Kikuchi K, Mizoguchi M, Yoshimoto K, Suzuki SO, Iwaki T, Obara M, Caeteren MV, Honda H : Differentiation of high-grade and low-grade diffuse gliomas by intravoxel incoherent motion MR imaging. *J Neuro Oncol* 18 : 132-141, 2016
2. Lin Y, Li J, Zhang Z, Xu Q, Zhou Z, Zhang Z, Zhang Y, Zhang Z : Comparison of Intravoxel Incoherent Motion Diffusion-Weighted MR Imaging and Arterial Spin Labeling MR Imaging in Gliomas. *J Biomed Res Int* 1-10, 2015
3. Federau C, O'Brien K, Meuli R, Hagmann P, Maeder P : Measuring brain perfusion with intravoxel incoherent motion (IVIM) : Initial clinical experience. *J Magn Reson Imaging* 39 : 624-632, 2014
4. Hu Y, Yan L, Wu L, Du L, Du P, Chen BY, Wang L, Wang SM, Han Y : Intravoxel incoherent motion diffusion-weighted MR imaging of gliomas : Efficacy in preoperative grading. *J Sci Rep* 4 : 1-7, 2014
5. Xu XQ, Choi YJ, Sung YS, Yoon RG, Jang WJ, Park JE, Heo YJ, Baek JH, Lee JH : Intravoxel Incoherent Motion MR Imaging in the Head and Neck : Correlation with Dynamic Contrast-Enhanced MR Imaging and Diffusion-Weighted Imaging. *Korean J Radiol* 17 : 641-649, 2016
6. Shen N, Zhao L, Jiang J, Jiang R, Su C, Zhang S, Tang X, Zhu W : Intravoxel incoherent motion diffusion-weighted imaging analysis of diffusion and microperfusion in grading gliomas and comparison with arterial spin labeling for evaluation of tumor perfusion. *J Magn Reson Imaging* 44 : 620-632, 2016
7. Xing Z, You RX, Li J, Liu Y, Cao DR : Differentiation of Primary Central Nervous System Lymphomas from High-Grade Gliomas by rCBV and Percentage of Signal Intensity Recovery Derived from Dynamic Susceptibility-Weighted Contrast-Enhanced Perfusion MR Imaging. *J Clin Neuro-radiol* 24 : 329-336, 2014
8. Federau C, Meuli R, O'Brien K, Maeder P, Hagmann P : Perfusion measurement in brain gliomas with Intravoxel incoherent motion MRI. *AJNR Am J Neuroradiol* 35 : 256-262, 2014
9. Puig J, Sanchez-Gonzalez J, Blasco G, Daunis-i-Estadella P, Federau C, Alberich-Bayarri A, Biarnes C, Nael K, Essig M, Jain R, Wintermark M, Pedraza S : Intravoxel incoherent motion metrics as potential biomarkers for survival in glioblastoma. *J PLoS One* 11 : 1-14, 2016
10. Barbier EL, Lamalle L, Decors M : Methodology of brain perfusion imaging. *J Magn Reson Imaging* 13 : 496-520, 2001
11. Toh CH, Wei KC, Chang CN, Ng SH, Wong HF : Differentiation of primary central nervous system lymphomas and glioblastomas : Comparisons of diagnostic performance of dynamic susceptibility contrast-enhanced perfusion mr imaging without and with contrast-leakage correction. *AJNR Am J Neuroradiol* 34 : 1145-1149, 2013
12. Kim YE, Choi SH, Lee ST, Kim TM, Park CK, Park SH, Kim IH : Differentiation between Glioblastoma and Primary Central Nervous System Lymphoma Using Dynamic

- Susceptibility Contrast-Enhanced Perfusion MR Imaging : Comparison Study of the Manual versus Semiautomatic Segmentation Method. *J Investig Magn Reson Imaging* 21 : 9-19 , 2017
13. Marco E, Shiroishi MS, Nguyen TB, Mark S, Provenzale JM, David E, Anzalone N, Arnd D, Alex R, Max W, Meng L : Perfusion MRI : The five most frequently asked technical questions *AJR Am J Roentgenol* 200 : 24-34, 2013
 14. Deibler AR, Pollock JM, Kraft RA, Tan H, Burdette JH, Maldjian JA : Arterial spin-labeling in routine clinical practice, part 3 : Hyperperfusion patterns. *AJNR Am J Neuroradiol* 29 : 1428-1435, 2008
 15. Federau C, Maeder P, O'Brien K, Browaeys P, Meuli R, Hagmann P : Quantitative Measurement of Brain Perfusion with Intravoxel Incoherent Motion MR Imaging. *J Radiology* 265 : 874-881, 2012
 16. Shim WH, Kim HS, Choi CG, Kim SJ : Comparison of apparent diffusion coefficient and intravoxel incoherent motion for differentiating among glioblastoma, metastasis, and lymphoma focusing on diffusion-related parameter. *J PLoS One* 10 : 1-13, 2015
 17. Suh CH, Kim HS, Lee SS, Kim N, Yoon HM, Choi GC, Kim SJ : Atypical imaging features of primary central nervous system lymphoma that mimics glioblastoma : Utility of Intravoxel incoherent motion MR imaging 272 : 504-513, 2014
 18. Yiping L, Kawai S, Jianbo W, Li L, Daoying G, Bo Y : Evaluation parameters between intra-voxel incoherent motion and diffusion-weighted imaging in grading and differentiating histological subtypes of meningioma : A prospective pilot study. *J Neurol Sci* 372 : 60-69, 2017
 19. Lu Y, Jacobus FA, Jansen JFA, Hilda ES, Stambuk HE, Gupta G, Lee N, Gonen M, Moreira A, Mazaheri Y, Patel SG, Deasy JO, Shah JP, Shukla-Dave A : Comparing primary tumors and metastatic nodes in head and neck cancer using intravoxel incoherent motion imaging : A preliminary experience. *J Comput Assist Tomogr* 37 : 346-352, 2013
 20. Le Bihan D : What can we see with IVIM MRI? *J Neuroimage* 187 : 56-67, 2019
 21. Wang J, Alsop DC, Li L, Listerud J, Gonzalez-At JB, Schnall MD, Detre JA : Comparison of quantitative perfusion imaging using arterial spin labeling at 1.5 and 4.0 Tesla. *J Magn Reson Med* 48 : 242-254, 2002
 22. Fabene PF, Farace P, Brambilla P, Andreone N, Cerini R, Pelizza L, Versace A, Rambaldelli G, Birbaumer N, Tansella M, Sbarbati A : Three-dimensional MRI perfusion maps : A step beyond volumetric analysis in mental disorders. *J Anat* 210 : 122-128, 2007
 23. Paschoal AM, Leoni RF, dos Santos AC, Paiva FF : Intravoxel incoherent motion MRI in neurological and cerebrovascular diseases. *J NeuroImage Clin* 20 : 705-714, 2018
 24. Knutsson L, Stahlberg F, Wirestam R : Absolute quantification of perfusion using dynamic susceptibility contrast MRI : pitfalls and possibilities. *J Magn Res Mater Phy* 23 : 1-21, 2010
 25. Kathleen MS, Melissa AP, Scott DR, Liu Y, Logan B, Muzy M, Swati DR, Da X, Yen Y, Jayashree KC, Thomas LC, Hoff B, Ross B, Cao Y, Madhava PA, Erickson B, Korfiatis P, Donglinger T, Bell L, Hu L, Kinahan P, Christopher CQ : Multi-site Concordance of DSC-MRI Analysis for Brain tumors : Results of a NCI Quantitative Imaging network collaborative project. *AJNR Am J Neuroradiol* 39 (6) : 1008-1016, 2018
 26. Boxerman JL, Schmainda KM, Weisskoff RM : Relative cerebral blood volume maps corected for Contrast Agent Extravasation Significantly Correlate with Glioma Tumor Grade, Whereas uncorrected map do not. *AJNR Am J Neuroradiol* 27 : 859-867, 2006
 27. Jiang J, Zhao L, Zhang Y, Zhang S, Yao Y, Qin Y, Wang C, Zhu W : Comparative analysis of arterial spin labeling and dynamic susceptibility contrast perfusion imaging for quantitative perfusion measurements of brain tumors. *J Int J Clin Exp Pathol* 7 : 2790-2799, 2014
 28. Petersen ET, Zimine I, Ho YC, Golay X : Non-invasive measurement of perfusion : a critical review of arterial spin labeling technique. *Br J Radiology* 79 : 688-701, 2006
 29. Warmuth C, Günther M, Zimmer C : Quantification of Blood Flow in Brain Tumors : Comparison of Arterial Spin Labeling and Dynamic Susceptibility-weighted Contrast-enhanced MR Imaging. *J Radiology* 228 : 523-532, 2003
 30. Iima M, Yano K, Kataoka M, Umehana M, Murata K, Kanao S, Togashi K, Le Bihan D : Quantitative non-gaussian diffusion and intravoxel incoherent motion magnetic resonance imaging : Differentiation of malignant and benign breast lesions. *J Invest Radiol* 50, 205-211, 2015